

## Negative index materials using simple short wire pairs

Jiangfeng Zhou,<sup>1</sup> Lei Zhang,<sup>1</sup> Gary Tuttle,<sup>1</sup> Thomas Koschny,<sup>2,3</sup> and Costas M. Soukoulis<sup>2,3</sup>

<sup>1</sup>*Department of Electrical and Computer Engineering and Microelectronics Research Center, Iowa State University, Ames, Iowa 50011, USA*

<sup>2</sup>*Ames Laboratory and Department of Physics and Astronomy, Iowa State University, Ames, Iowa 50011, USA*

<sup>3</sup>*Institute of Electronic Structure and Laser-FORTH, and Department of Materials Science and Technology, University of Crete, Heraklion, Crete, Greece*

(Received 27 October 2005; published 4 January 2006)

Negative refraction is currently achieved by a combination of artificial “electric atoms” (metallic wires with negative electrical permittivity  $\epsilon$ ) and artificial “magnetic atoms” (split-ring resonators with negative magnetic permeability  $\mu$ ). Both  $\epsilon$  and  $\mu$  must be negative at the same frequency, which is not easy to achieve at higher than THz frequencies. We introduce improved and simplified structures made of periodic arrays of pairs of short metal wires and continuous wires that offer a potentially simpler approach to building negative index materials. Using simulations and microwave experiments, we have investigated the negative index  $n$  properties of short wire-pair structures. We have measured experimentally both the transmittance and the reflectance properties and found unambiguously that  $n < 0$ . The same is true for  $\epsilon$  and  $\mu$ . Our results show that short wire-pair arrays can be used very effectively in producing materials with negative refractive indices.

DOI: [10.1103/PhysRevB.73.041101](https://doi.org/10.1103/PhysRevB.73.041101)

PACS number(s): 41.20.Jb, 42.25.Bs, 42.70.Qs, 78.20.Ci

The first demonstration of a left-handed (LH) material<sup>1,2</sup> by the UCSD group, in 2000, following the work by Pendry *et al.*,<sup>3,4</sup> underscores the relevance of utilizing structured materials to create electromagnetic response not available in naturally occurring materials. This LH material made use of an array of conducting, nonmagnetic elements to achieve a negative effective permeability,  $\mu(\omega)$ , and an array of conducting continuous wires to achieve a negative effective permittivity,  $\epsilon(\omega)$ , the simultaneous combination of which had never before been observed in any previously known material. While a number of theoretical concerns were raised shortly after the reporting of these experiments, subsequent measurements<sup>5–8</sup> on similar metamaterials have firmly established the foundation of negative refraction. LH materials will display unique “reversed” electromagnetic properties, as discussed by Veselago<sup>9</sup> long before such materials existed. All of these reversals stem from the fact that a LH material is characterized by a negative refractive index, a property that does not exist in any known natural material, and represents a new regime of physics.

In the past few years there has been ample proof for the existence of negative index materials (NIMs) in the GHz frequency range.<sup>1–8</sup> All NIM implementations to date have utilized the topology proposed by Pendry, consisting of split-ring resonators (SRRs) (rings with gaps, providing the negative  $\mu$ ) and continuous wires (providing the negative  $\epsilon$ ). Many groups were able to fabricate<sup>1,2,5–8</sup> NIMs with an index of refraction  $n = -1$  with losses of less than 1 dB/cm. Recently, different groups observed indirectly<sup>10–13</sup> negative  $\mu$  at the THz region. In most of the THz experiments<sup>10–12</sup> only one layer of SRRs was fabricated on a substrate and the transmission,  $T$ , was measured only for propagation perpendicular to the plane of the SRRs, exploiting the coupling of the electric field to the magnetic resonance of the SRR via asymmetry.<sup>11</sup> This way it is not possible to drive the magnetic permeability negative. Also, no negative  $n$  with a small

imaginary part has been observed yet at the THz region. One reason is that it is very difficult to measure with the existing topology of SRRs and continuous wires both the transmission,  $T$ , and reflection,  $R$ , along the direction parallel to the plane of the SRRs. So there is a need for alternative, improved, and simplified designs that can be easily fabricated and experimentally characterized. Currently, there is much interest in pushing the frequency range for NIM behavior into the infrared and optical regions of the spectrum.

Designing a material structure to have an effective negative refractive index can be achieved by having simultaneously negative permeability and negative permittivity over some range of frequencies. Nearly all negative index materials that have been investigated up until this point have been based on the use of split-ring resonators, which have been described in detail elsewhere.<sup>1,2,5,6</sup> Conceptually, an SRR starts with a loop of wire that provides an inductive response to an incident field. Cutting out a short section of the loop leads to a capacitive gap. The inductance ( $L$ ) and capacitance ( $C$ ) together form an LC resonator, with resonance frequency  $\omega_R = 1/\sqrt{LC}$ . For an electromagnetic wave incident with its wave vector parallel to the plane of the SRR and the magnetic field perpendicular to the SRR, the response at the resonance frequency will be as if the SRR had a negative permeability. To build a negative index material, an array of SRRs is combined with a grid of continuous metal wires, which is known to exhibit a negative permittivity,<sup>3</sup> so that the two effects together lead to NIM behavior.

Recent theoretical work<sup>14</sup> has shown that using pairs of finite length wires would not only allow replacing the SRRs as magnetic resonators but could also give simultaneously a negative  $\epsilon$  in the same frequency range, and therefore a negative  $n$ , without the need for additional continuous wires. The condition to obtain simultaneously negative  $\mu$  and  $\epsilon$  by pairs of finite metallic wires is very restrictive. Recent experiments<sup>15</sup> have not shown evidence of negative  $n$  in the

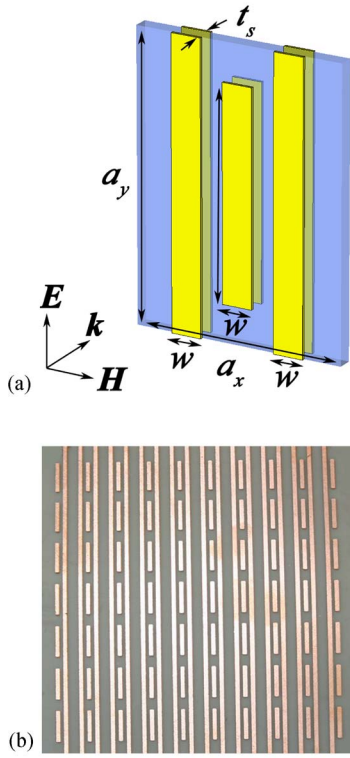


FIG. 1. (Color online) (a) Schematic representation of one unit cell of the wire-pair structure. (b) Photograph of one side of a fabricated microwave-scale wire-pair sample.

short wire-pair cases that were studied. This is in contrast with the claims<sup>16</sup> that one can get negative  $n$  at THz frequencies.

In this Communication, we report our investigations of wire-pair structures as alternatives to conventional SRR-based NIMs. The basic structure of a single unit cell of the wire-pair NIM is shown in Fig. 1(a). In the wire-pair arrangement, the conventional SRR is replaced with a pair of short parallel wires and the continuous wires are preserved. The short wire pair consists of a pair of metal patches separated by a dielectric spacer of thickness  $t_s$ . In essence, the short wire pair is a “two-gap” SRR that has been flattened to result in the wire-pair arrangement.<sup>15</sup> For an electromagnetic wave incident with wave vector and field polarization as shown in Fig. 1(a), the short wire pair will exhibit both inductive (along the wires) and capacitive (between the upper and lower adjacent ends of the short wires) behavior and will possess magnetic resonance providing a negative permeability. The inductance  $L$  of a short wire pair is approximately given, as inductance of parallel plates, by  $L = \mu_0(l \cdot t_s)/w$ , where  $l$  is the length of the short wires,  $w$  is the width, and  $t_s$  is the separation distance between the short wires. The capacitance  $C$  of the short wire pairs can be written as the two plate capacitor formula for the upper and lower halves of the short wire pair  $C = \epsilon_r \epsilon_0(l \cdot w)/(4t_s)$ , where  $\epsilon_0$  is permittivity in vacuum and  $\epsilon_r$  is the relative dielectric constant of the region between the wires. Then the frequency of the magnetic resonance is

$$f_m = \frac{1}{2\pi\sqrt{LC}} = \frac{1}{\pi l \sqrt{\epsilon_r \epsilon_0 \mu_0}} = \frac{c_0}{\pi l \sqrt{\epsilon_r}}, \quad (1)$$

where  $c_0$  is the speed of light in vacuum. From (1), the magnetic-resonance frequency is inversely proportional to the length of the wires in the pairs, but does not depend on the wire widths or separation between the wires. Resonance frequencies determined by detailed simulations of short wire-pair structures with various combinations of parameters ( $l, w, t_s$ ) show good agreement with the simple formula above. However, our simulations have shown that it is difficult to obtain a negative  $n$  with only pairs of short wires. This is because the electric resonance of the short wires is usually well above the magnetic-resonance frequency, thus preventing  $\epsilon$  and  $\mu$  from becoming simultaneously negative. To realize NIM behavior, the short wire pairs must be combined with a continuous wire grid that provides the extra negative permittivity. In our structure, two additional continuous wires are placed on either side of the short wire pairs. Repeating this basic structure periodically in the  $x$ ,  $y$ , and  $z$  directions would result in a NIM structure.

The short wire-pair arrangement has a distinct advantage over conventional SRRs. Since all of the features of the wire-pair NIM lie in parallel planes, conventional microfabrication techniques can be used to build the structures. In particular, the methods for making complex multilevel interconnects in integrated circuits could be applied directly to making wire-pair NIMs.

To examine the potential usefulness of wire-pair structures as NIMs, we characterized the properties of the wire pair of Fig. 1(a) using simulations and microwave measurements, and then used these results to determine the expected properties of NIMs built from the wire-pair building blocks. Simulations of wire-pair structures were done with CST Microwave Studio (Computer Simulation Technology GmbH, Darmstadt, Germany), which uses a finite-difference time-domain method to determine reflection and/or transmission properties of metallodielectric structures. In the simulations, the dielectric properties of the metal patches were handled with a frequency dependent Drude model. The detailed calculations were used to determine reflection and transmission coefficients from a single unit cell. Experimental transmission and reflection data were obtained by building and measuring microwave-frequency versions of the wire-pair structures. These were fabricated using Rogers 5880 printed circuit board stock with a dielectric layer thickness of  $254 \mu\text{m}$  and a listed relative dielectric constant of 2.53. The circuit board was coated on both sides with  $10\text{-}\mu\text{m}$ -thick layers of copper. The copper was formed in the wire-pair patterns using conventional photolithography techniques. For the samples reported here (both simulations and experiments), the widths of all metal lines were 1 mm. The length of the short wire pairs was 7 mm, and the unit-cell size was  $9.5 \times 7 \times 2.274 \text{ mm}^3$ . The total sample size was  $7 \times 10 \times 1$  unit cells, resulting in approximately square samples. A photograph of one side of a complete sample is shown in Fig. 1(b). With these patterned dimensions on the printed circuit board material, the resonances for NIM behavior were expected to occur near 13.7 GHz.

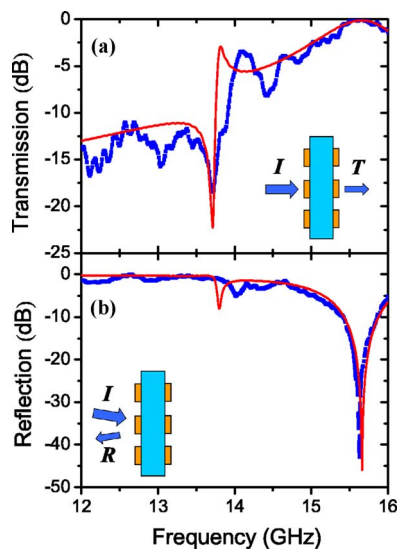


FIG. 2. (Color online) Simulated (red thin line) and measured (blue thick-dotted line) response to electromagnetic radiation incident on the wire-pair structures: (a) transmission, (b) reflection.

Transmission and reflection properties of a single-layer structure were measured over the frequency range of 12–16 GHz using a network analyzer (HP 8510) and a pair of standard gain horn antennas serving as a source and receiver, as shown in the insets of Fig. 2. In the transmission measurements, the microwaves were incident normal to the sample surface. This is a tremendous simplification relative to the conventional SRRs and wires where the incident electromagnetic waves have to propagate parallel to the sample surface. With the conventional orientation of the SRRs, it is almost impossible to do these types of measurements at the THz region, since only single-layer samples are usually fabricated.<sup>10,11</sup> Transmission measurements were calibrated to the transmission between the horns with the sample removed. The reflection measurements were done by placing the source and receiving horns on the same side of the sample and bouncing the microwave signal off the sample. The source and receiver horns were each inclined with an angle of about  $7.5^\circ$  with respect to normal on the sample surface. The reflection measurement was calibrated using a sample-sized sheet of copper as a reflecting mirror. In both measurements, the electric field of the incident wave was polarized parallel to the long dimension of the wires. (For perpendicular polarization, the transmission was nearly 100%, independent of frequency in the resonance region, and reflection was essentially zero.)

The calculated and measured transmission spectra are shown in Fig. 2(a). Figure 2(b) shows the calculated and measured reflection spectra. There is good qualitative agreement between simulations and measurements. The measured spectrum does show resonance peaks and valleys due to reflections between the receiving horn and the sample. Also, there is a distinct frequency difference between critical points in the two sets of curves. The frequencies of the measured transmission resonance peak and the corresponding reflection dip near 14.0 GHz are about 2% higher than in the

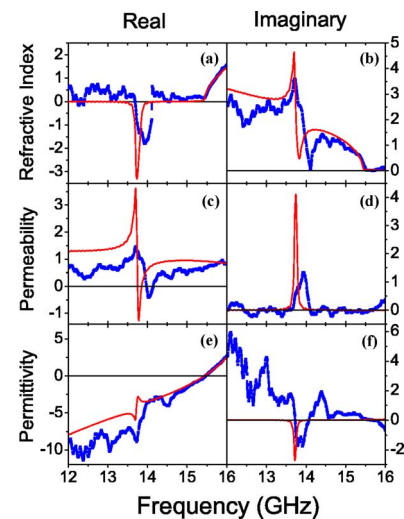


FIG. 3. (Color online) Extracted electromagnetic properties of a periodic array of wire-pair unit cells, using the simulated (red thin line) and measured (blue thick-dotted line) data of Fig. 2. Real (a) and imaginary (b) parts of the refractive index. Real (c) and imaginary (d) parts of the permeability. Real (e) and imaginary (f) part of the permittivity. The negative-index behavior can be seen clearly near 14 GHz in (a).

simulations. There are three potential causes for the shift: (1) The external resonances in the measurements may be masking the true peak (dip) in the measured data. (2) The actual dielectric constant of the circuit board material may be slightly lower than the value used in the simulations. (3) The wires on the front and back of the dielectric layer may be misaligned slightly, which would have the same effect as shortening the wires. The dip in the reflection at 15.7 GHz is due to the fact that the sample impedance  $z=1$  at that frequency, and so no reflection is possible.

Using the transmission and reflection results from a single layer, we can extract the effective refractive index that would result if a periodic multilayer sample were built using the single-layer structure as a building block. The details of the numerical retrieval procedure have been described elsewhere.<sup>17–19</sup> In performing the retrieval, we have assumed a  $z$ -direction size of the unit cell of 2.274 mm. This interlayer spacing is an adjustable parameter in the retrieval process. Smaller spacing would lead to stronger negative index features in the periodic structure, as long as the distance between the short wires is small compared to the length of the unit cell, but may also result in more complicated fabrication procedures in building a multilayer structure. In choosing 2.274 mm as the separation distance for the numerical extraction, we attempted to strike a balance between good negative index properties and having a separation distance that is in line with the other feature sizes of the structure. The extracted permittivity, permeability, and refractive index are shown in the various parts of Fig. 3. The plots show that the real part of the permittivity is negative over most of the measured range.<sup>20</sup> The real part of the permeability is negative over a resonance band near 13.8 GHz for the simulation and at about 14.0 GHz for the measurement. Notice also that

the product of  $\text{Im}(\varepsilon)$  and  $\text{Im}(\mu)$  is negative. This is a well known and real effect, which comes from the periodic effects of the retrieval procedure.<sup>11</sup> It is not relevant to the discussion of our results. The extracted real part of the refractive index is negative<sup>21</sup> over a narrow band at 13.8 GHz for the simulations and 14.0 GHz in the experiments, dipping as low as  $-2$  using measured data, and to less than  $-3$  from the simulation. The ratio of the imaginary part of  $n$  to the real part of  $n$  is  $\frac{1}{4}$ , which means that we have left-handed propagation with  $\varepsilon$ ,  $\mu$ , and  $n$  negative. Our preliminary numerical results show that if our structure scales down by a factor of 200, it will give a negative index of refraction at THz frequencies, with both  $\varepsilon$  and  $\mu$  negative.

These results show clearly the viability of using short wire pairs to build negative index materials, if combined with additional continuous wires. It is likely that modifications of the basic structure studied here may improve or alter the NIM properties. Also, wire-pair arrangements with significantly different geometries may lead to negative index materials. The relative ease of fabricating wire-pair structures may hasten the development of NIMs working at optical wavelengths.

We gratefully acknowledge the support of Ames Laboratory, which is operated by Iowa State University under Contract No. W-7405-Eng-82, EU FET project DALHM, and DARPA (Contract No. HR0011-05-C-0068).

- <sup>1</sup>D. R. Smith, W. J. Padilla, D. C. Vier, S. C. Nemat-Nasser, and S. Schultz, *Phys. Rev. Lett.* **84**, 4184 (2000).
- <sup>2</sup>R. A. Shelby, D. R. Smith, and S. Schultz, *Science* **292**, 77 (2001).
- <sup>3</sup>J. B. Pendry, A. J. Holden, D. J. Robbins, and W. J. Stewart, *IEEE Trans. Microwave Theory Tech.* **47**, 2075 (1999); J. B. Pendry, A. J. Holden, W. J. Stewart, and I. Youngs, *Phys. Rev. Lett.* **76**, 4773 (1996).
- <sup>4</sup>J. B. Pendry, *Phys. Rev. Lett.* **85**, 3966 (2000).
- <sup>5</sup>C. G. Parazzoli, R. B. Gregor, K. Li, B. E. C. Koltenbah, and M. Tanielian, *Phys. Rev. Lett.* **90**, 107401 (2003); K. Li, S. J. McLean, R. B. Gregor, C. G. Parazzoli, and M. H. Tanielian, *Appl. Phys. Lett.* **82**, 2535 (2003).
- <sup>6</sup>M. Bayindir, K. Aydin, E. Ozbay, P. Markos, and C. M. Soukoulis, *Appl. Phys. Lett.* **81**, 120 (2002); K. Aydin, K. Guven, M. Kafesaki, L. Zhang, C. M. Soukoulis, and E. Ozbay, *Opt. Lett.* **29**, 2623 (2004).
- <sup>7</sup>E. Cubukcu, K. Aydin, E. Ozbay, S. Foteinopoulou, and C. M. Soukoulis, *Nature (London)* **423**, 604 (2003); *Phys. Rev. Lett.* **91**, 207401 (2003).
- <sup>8</sup>P. V. Parimi, W. T. T. Lu, P. Vodo, and S. Sridhar, *Nature (London)* **426**, 404 (2003).
- <sup>9</sup>V. G. Veselago, *Sov. Phys. Usp.* **10**, 509 (1968).
- <sup>10</sup>T. J. Yen, W. J. Padilla, N. Fang, D. C. Vier, D. R. Smith, J. B. Pendry, D. N. Basov, and X. Zhang, *Science* **303**, 1494 (2004).
- <sup>11</sup>S. Linden, C. Enkrich, M. Wegener, J. F. Zhou, T. Koschny, and C. M. Soukoulis, *Science* **306**, 1351 (2004).
- <sup>12</sup>S. Zhang, W. J. Fa, B. K. Minhas, A. Frauenglass, K. J. Malloy, and S. R. J. Brueck, *Phys. Rev. Lett.* **94**, 037402 (2005).
- <sup>13</sup>N. Katsarakis, G. Konstantinidis, A. Kostopoulos, R. S. Penciu, T. F. Gundogdu, M. Kafesaki, E. N. Economou, T. Koschny, and C. M. Soukoulis, *Opt. Lett.* **30**, 1348 (2005).
- <sup>14</sup>V. A. Podlovsk, A. K. Sarychev, and V. M. Shalaev, *J. Nonlinear Opt. Phys. Mater.* **11**, 65 (2002); *Opt. Express*, **11**, 735 (2003).
- <sup>15</sup>G. Dolling, C. Enkrich, M. Wegener, J. F. Zhou, C. M. Soukoulis, and S. Linden, *Opt. Lett.*, **30**, 3198 (2005).
- <sup>16</sup>V. M. Shalaev, W. Cai, U. K. Chettiar, H. K. Yuan, A. K. Sarychev, V. P. Drachev, and A. V. Kildishev, *Opt. Lett.* **30**, 3356 (2005).
- <sup>17</sup>D. R. Smith, S. Schultz, P. Markos, and C. M. Soukoulis, *Phys. Rev. B* **65**, 195104 (2002).
- <sup>18</sup>D. R. Smith, D. C. Vier, Th. Koschny, and C. M. Soukoulis, *Phys. Rev. E* **71**, 036617 (2005).
- <sup>19</sup>Th. Koschny, P. Markos, E. N. Economou, D. R. Smith, D. C. Vier, and C. M. Soukoulis, *Phys. Rev. B* **71**, 245105 (2005).
- <sup>20</sup>We have also done experiments and simulations for samples with only pairs of short wires. For this case both the experiments and the simulations have shown that indeed  $\mu$  is negative, however  $\varepsilon$  is not negative in this region and therefore  $n$  is also not negative. The extra continuous wires are needed to drive  $\varepsilon$  to become negative, without changing the magnetic response shown in Fig. 3(c).
- <sup>21</sup>In lossy materials it is possible to have the real part  $n$  be negative, without having the real parts of  $\varepsilon$  and  $\mu$  simultaneously negative. This is the case of the recent work of S. Zhang, W. J. Fan, N. C. Panoiu, K. J. Malloy, R. M. Osgood, and S. R. J. Brueck. [*Phys. Rev. Lett.* **95**, 137404 (2005)]. This can happen if the imaginary parts of  $\varepsilon$  and  $\mu$  are sufficiently large, because in a lossy material  $n = n' + in''$ , and we also have that  $n = \varepsilon z$  and  $z = \sqrt{\mu/\varepsilon}$ . After some algebra we obtain that  $n' = \varepsilon' z' - \varepsilon'' z''$  and  $z = \sqrt{\mu' \varepsilon' + \mu'' \varepsilon'' / \varepsilon'^2 + i(\mu'' \varepsilon' - \mu' \varepsilon'' / \varepsilon'^2)}$ , so it is possible to have  $n' < 0$ , provided that  $\varepsilon'' z'' > \varepsilon' z'$ . In this scenario, which occurs at the low-frequency side of the  $n' < 0$  region in Fig. 3(a), however, the imaginary parts lead to dominant losses such that we have a transmission gap with some negative phase shift rather than LH transmission (with some losses). This type of negative  $n$  should not be considered LH behavior. In our experiments, although we have considerable imaginary parts, the behavior is still dominated by the negative real part of  $n$  at the high-frequency side where we find the LH behavior. As one can see from the experimental data of Figs. 3(a) and 3(b), we obtain  $n'/n'' = 3.5$  at  $n' = -1$ , which ratio improves to  $\sim 15$  for  $n' = -0.76$ . The simulation data gives at least  $n'/n'' \approx 3.0$  for  $n' = -1.7$ .

## 射频和天线设计培训课程推荐

易迪拓培训([www.edatop.com](http://www.edatop.com))由数名来自于研发第一线的资深工程师发起成立,致力并专注于微波、射频、天线设计研发人才的培养;我们于 2006 年整合合并微波 EDA 网([www.mweda.com](http://www.mweda.com)),现已发展成为国内最大的微波射频和天线设计人才培养基地,成功推出多套微波射频以及天线设计经典培训课程和 ADS、HFSS 等专业软件使用培训课程,广受客户好评;并先后与人民邮电出版社、电子工业出版社合作出版了多本专业图书,帮助数万名工程师提升了专业技术能力。客户遍布中兴通讯、研通高频、埃威航电、国人通信等多家国内知名公司,以及台湾工业技术研究院、永业科技、全一电子等多家台湾地区企业。

易迪拓培训课程列表: <http://www.edatop.com/peixun/rfe/129.html>



### 射频工程师养成培训课程套装

该套装精选了射频专业基础培训课程、射频仿真设计培训课程和射频电路测量培训课程三个类别共 30 门视频培训课程和 3 本图书教材;旨在引领学员全面学习一个射频工程师需要熟悉、理解和掌握的专业知识和研发设计能力。通过套装的学习,能够让学员完全达到和胜任一个合格的射频工程师的要求...

课程网址: <http://www.edatop.com/peixun/rfe/110.html>

### ADS 学习培训课程套装

该套装是迄今国内最全面、最权威的 ADS 培训教程,共包含 10 门 ADS 学习培训课程。课程是由具有多年 ADS 使用经验的微波射频与通信系统设计领域资深专家讲解,并多结合设计实例,由浅入深、详细而又全面地讲解了 ADS 在微波射频电路设计、通信系统设计和电磁仿真设计方面的内容。能让您在最短的时间内学会使用 ADS,迅速提升个人技术能力,把 ADS 真正应用到实际研发工作中去,成为 ADS 设计专家...



课程网址: <http://www.edatop.com/peixun/ads/13.html>



### HFSS 学习培训课程套装

该套课程套装包含了本站全部 HFSS 培训课程,是迄今国内最全面、最专业的 HFSS 培训教程套装,可以帮助您从零开始,全面深入学习 HFSS 的各项功能和在多个方面的工程应用。购买套装,更可超值赠送 3 个月免费学习答疑,随时解答您学习过程中遇到的棘手问题,让您的 HFSS 学习更加轻松顺畅...

课程网址: <http://www.edatop.com/peixun/hfss/11.html>

## CST 学习培训课程套装

该培训套装由易迪拓培训联合微波 EDA 网共同推出,是最全面、系统、专业的 CST 微波工作室培训课程套装,所有课程都由经验丰富的专家授课,视频教学,可以帮助您从零开始,全面系统地学习 CST 微波工作的各项功能及其在微波射频、天线设计等领域的设计应用。且购买该套装,还可超值赠送 3 个月免费学习答疑...

课程网址: <http://www.edatop.com/peixun/cst/24.html>



## HFSS 天线设计培训课程套装

套装包含 6 门视频课程和 1 本图书,课程从基础讲起,内容由浅入深,理论介绍和实际操作讲解相结合,全面系统的讲解了 HFSS 天线设计的全过程。是国内最全面、最专业的 HFSS 天线设计课程,可以帮助您快速学习掌握如何使用 HFSS 设计天线,让天线设计不再难...

课程网址: <http://www.edatop.com/peixun/hfss/122.html>

## 13.56MHz NFC/RFID 线圈天线设计培训课程套装

套装包含 4 门视频培训课程,培训将 13.56MHz 线圈天线设计原理和仿真设计实践相结合,全面系统地讲解了 13.56MHz 线圈天线的工作原理、设计方法、设计考量以及使用 HFSS 和 CST 仿真分析线圈天线的具体操作,同时还介绍了 13.56MHz 线圈天线匹配电路的设计和调试。通过该套课程的学习,可以帮助您快速学习掌握 13.56MHz 线圈天线及其匹配电路的原理、设计和调试...

详情浏览: <http://www.edatop.com/peixun/antenna/116.html>



### 我们的课程优势:

- ※ 成立于 2004 年,10 多年丰富的行业经验,
- ※ 一直致力并专注于微波射频和天线设计工程师的培养,更了解该行业对人才的要求
- ※ 经验丰富的一线资深工程师讲授,结合实际工程案例,直观、实用、易学

### 联系我们:

- ※ 易迪拓培训官网: <http://www.edatop.com>
- ※ 微波 EDA 网: <http://www.mweda.com>
- ※ 官方淘宝店: <http://shop36920890.taobao.com>